Research in Pharmaceutical Sciences, April 2022; 17(2): 143-152
Received: 29-07-2021
Peer Reviewed: 14-08-2021
Revised: 29-08-2021
Accepted: 04-09-2021
Published: 15-01-2022

School of Pharmacy & Pharmaceutical Sciences
Isfahan University of Medical Sciences

Original Article

Facile and fast preparation of layered double hydroxide as a nanocarrier for ascorbic acid under ultrasonic irradiation

Parvin Asadi[1,2,*], Elahe Khodamoradi[1], and Mohammad Dinari[3]

[1]*Department of Medicinal Chemistry, School of Pharmacy and Pharmaceutical Sciences, Isfahan University of Medical Sciences, Isfahan, I.R. Iran.*
[2]*Isfahan Pharmaceutical Sciences Research Center, School of Pharmacy and Pharmaceutical Science, Isfahan University of Medical Sciences, Isfahan, I.R. Iran.*
[3]*Department of Chemistry, Isfahan University of Technology, Isfahan, I.R. Iran.*

Abstract

Background and purpose: Layered double hydroxides (LDHs) as inorganic materials are being used in controlled release and drug delivery systems. These materials are more stable than conventional drug carriers. In this investigation, Mg/Al-ascorbic acid (ASA) LDH nanohybrid was synthesized by ultrasonic-assisted co-deposition techniques.

Experimental approach: In this study, Mg/Al-LDH to adsorption of ASA anions from the alkaline solution was assembled by a facile coprecipitation technique. During this process, ultrasonic irradiation was used to increase the rate of ion exchange between LDH and ASA. The intercalated-layered structure was characterized by FT-IR spectroscopy, XRD, thermogravimetric analysis, field emission SEM, and TEM. ASA releasing from Mg/Al-ASA LDH nanohybrid was carried out in incubation sodium carbonate solution (0.5 M) at 35 °C using UV-Vis absorbance analysis at λ = 265 nm

Findings/Results: The used techniques confirmed the structure of Mg/Al-LDH and indicated successful intercalation of ASA into the interlayer galleries of the LDH host. The obtained results also have shown that Mg/Al-ASA LDH nanohybrid was generated with an average diameter size of 25 nm and narrow size distribution. Analysis of the release profiles using several kinetic models suggested that the first-order rate model is the most appropriate for describing the release of ASA from Mg/Al-LDH which means the amount of drug released is proportional to the amount of remaining drug in the matrix. Thus, the amount of activity released tends to decrease in function of time.

Conclusion and implications: The results showed that LDHs are good host materials to preserve the biomolecule and modify its release rate and bioavailability.

Keywords: Ascorbic acid; Controlled release; Coprecipitation; Layered double hydroxide; Ultrasonic irradiation.

INTRODUCTION

Layered double hydroxides (LDH) or hydrotalcite clay is organized into a broad family of synthetic 2D-nanostructured materials (1,2). They have 2D structure of layers shaped by trivalent and divalent cations carve-up by water and anions molecules with the general formula $[M_{1-x}^{2+}M_x^{3+}(OH)_2]^{x+}(A_{x/n}^{n-}).mH_2O$, where M^{2+} and M^{3+} usually stand for the divalent and trivalent metal ions, A^{n-} is an anion in the interlamellar region, *m* is the amount of H_2O present in the same region, and x constant value usually corresponds to $0.2 < x < 0.4$ in forming a new LDH phase (3-8).

Among the nanoparticles, LDHs as the bioinorganic hybrid systems have recently received outstanding attention in the fields of drug carriers and catalysts, *etc* (9-13).

*Correspondence author: P. Asadi
Tel: +98-3137927109, Fax: +98-3136680011
Email: asadi@pharm.mui.ac.ir

Access this article online

Website: http://rps.mui.ac.ir

DOI: 10.4103/1735-5362.335173

The incorporation of the therapeutic guest molecules into layered inorganic constituents, as hydrotalcite or other LDH, can act as a reservoir or chemical flask jacket for biomolecules guests (14-16). The framework of the LDH structure can protect biomaterials against harsh external conditions and cause noticeable longevity and stability in them in unsuitable conditions physically, chemically, and biologically. Furthermore, the LDHs by controlled release drugs can be decreased the undesirable effects caused by excessive dosage. (17-21).

Various therapeutic molecules and bio-functionalized molecules such as ascorbic acid (ASA) were successfully intercalated into the gallery space of LDH, which presents a new route to safe preservation and controlled release of biomolecules (22-24). Vitamin C or ASA, due to having outstanding properties, can assist in reducing the tumor cell, prohibit scurvy, protect tissues from free radical damage, supports the cardiovascular system, and decrease low-density lipoprotein cholesterol in the plasma (25). Nevertheless, the various environmental conditions such as light, moisture, metal ions, heat, and base can cause denaturation and decomposition of physicochemical properties in ASA. Mg-Al LDH as an antacid and anti-pepsin agent is quite biocompatible, so it can be used as a good reservoir to protect ASA against decomposition (26-30).

The sonochemical technique has shown an economical and suitable approach for the synthesis of LDHs (31-35). In this method, in the effect of acoustic waves, a series of mechanochemical impacts, such as high shear forces, shock waves, and microbubbles, are produced in the liquid and are made the state of too high temperatures and pressures, so-called hot spots. These local conditions are accountable for inducing dramatic changes in product morphology and dispersion of particles (31). According to the previous works, the ultrasonic-assisted route immensely increases anion-exchange capability, enhances the porosity and surface morphology of the LDH, and also improved the metal-ion distribution on the surface (32-35).

In this context, preparation hydrotalcite containing Mg^{2+} and Al^{3+} in the brucite-like layers and the interaction of ASA into them by a simple coprecipitation technique under ultrasonic irradiation is reported. It is believed that by the use of ultrasonic irradiation, the intercalation rate of ASA guests into the space of the LDH will be improved. The LDH structure and thermal behavior of ASA located in the interlayer gallery of LDHs are examined by transmission electron microscopy (TEM), field emission scanning electron microscopy (FE-SEM), X-ray diffraction (XRD), thermogravimetric analysis (TGA), and Fourier-transform infrared (FT-IR). In final, the quantitative determination of the intercalated ASA and the deintercalation behavior of ASA from the host supramolecular clays was investigated by the ion exchange method with CO_3^{2-} using ultraviolet-visible (UV-Vis) absorbance analysis.

MATERIALS AND METHODS

All solvents and chemicals were supplied by Aldrich and Merck Chemical Co. Sodium hydroxide, $Mg(NO_3)_2 \cdot 6H_2O$, and $Al(NO_3)_3 \cdot 9H_2O$ were used without further purification. The deionized water was used during all experiments.

The FT-IR spectra in the range of 4000-400 cm^{-1} on the Jasco-680 (Japan) spectrophotometer were obtained with a nominal resolution of 4 cm^{-1}. Elemental analyses were performed with a LECO CHNS-932. Aluminum and magnesium contents were determined in triplicate by inductively coupled plasma optical emission spectroscopy (ICP OES) on a Spectro Arcos spectrometer. The XRD patterns of samples were recorded using a Philips Xpert MPD diffractometer equipped with graphite-filtered CuKα radiation (λ = 0.151418 nm) in 2θ range of 5-80° at the scanning speed of 0.05°/min. The surface morphology of the LDH-ASA was observed using FE-SEM (HITACHI (S-4160); Tokyo, Japan) and TEM (Philips CM 120; Eindhoven, Netherland) microscope with an accelerating voltage of 100 kV. The thermal stability of the Mg/Al-ASA LDH nanohybrid was carried out by recording TGA and performed with an STA503 win TA at a heating rate of 20 °C/min from 25 °C to 800 °C under an argon flow.

An SW-3H ultrasonic homogenizer device with a power and frequency wave of 100 W and 25 Hz was utilized in the preparation of the samples. The UV-vis spectra of Mg/Al-ASA LDH nanohybrid were measured on UV/Vis/NIR spectrophotometer, JASCO, V-570 (Tokyo, Japan), with the liquid sample in the 265 nm.

Preparation of hydrotalcite-intercalated drug

A salt solution was prepared by adding 10 mL of deionized water to 0.37 g (1 mmol) $Al(NO_3)_3.9H_2O$ and 0.5 g (2 mmol) $Mg(NO_3)_3.6H_2O$. The obtained solution was slowly added within 10 mL of an alkaline solution containing the 0.258 g ASA in pH = 9. The reaction was carried out at room temperature during vigorous magnetic stirring. During this operation, the required amount of 1 M NaOH was added drop-wise into a mixed aqueous solution until maintaining the pH at a value close to 9. The resultant light-red precipitate was ultrasonicated in a water bath for 3 h under N_2 flow. The suspension was then collected by centrifugation and repeatedly washed by redispersion in deionized water followed by centrifugation and air-dried for 8 h at 50 °C. Mg/Al-LDH without ASA and Mg/Al-ASA LDH with 1 h sonication were prepared by a similar procedure.

Drug release studies by ion-exchange method

To investigate the release behavior of ASA anions from nanohybrid by ion exchange, 50 mL of 0.05 M Na_2CO_3 solution was placed in a 100 mL beaker together with 0.1 g of Mg/Al-ASA LDH and was stirring vigorously at a constant temperature of 35 °C. Then, 7 mL of suspension was withdrawn and was separated by centrifugation at a different time to determine the amount of drug released by UV-vis absorption at wavelengths 265 nm. For every aliquot removed, 7 mL fresh buffer was added. The amount of ASA obtained at every interval was quantified using the UV-Vis.

RESULTS

Hydrotalcite-intercalated ASA was prepared through the co-precipitation method by using ultrasonic irritation according to Scheme 1. To confirm the presence of ASA anion in LDHs, release profiles of Mg/Al-ASA LDH in deionized water at 265 nm belonging to π-π^* transition of ASA was performed (Fig. 1) which showed a strong absorption peak at this wavelength. Chemical structures of synthesized intercalated LDH were confirmed by IR, XRD, and CHN methods. The results of the analysis are as below:

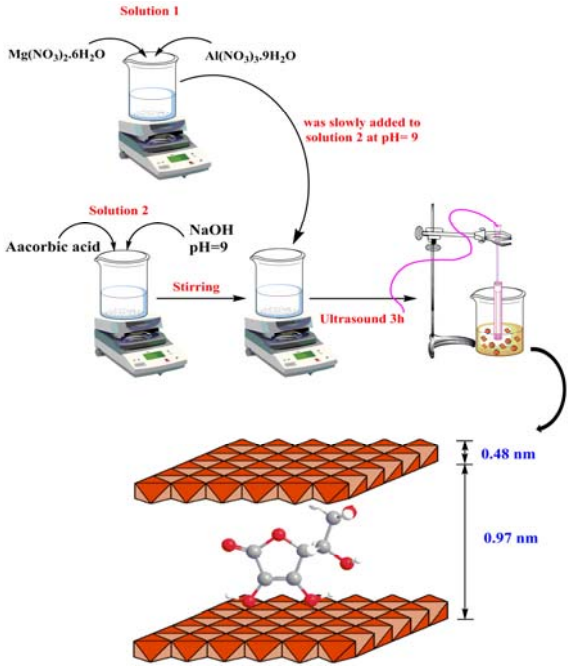

Scheme 1. Schematic illustration of the synthesis and possible interlayer arrangement of ascorbic acid in the Mg/Al layered double hydroxides.

FT-IR spectrum of neat ASA, LDH-ASA after 1 h ultra, LDH-ASA after 3h ultra, and also LDH-CO_3 are shown in Fig. 2. Although FT-IR spectroscopy is not a precise diagnostic technique for LDH, it is useful in characterizing the interaction between the interlayer anions and the basal sheets described in the discussion part.

Figure 3 shows the XRD pattern of the neat LDH and LDH/ASA samples synthesized at pH = 9 under ultrasonic irradiation. The samples showed the hydrotalcite-like characteristic reflections of d_{003} = 0.76 and d_{006} = 0.38 nm peaks. The XRD patterns of Mg/Al-ASA LDH displayed sharp and symmetric (003) and (006) Bragg reflection shifts to lower 2θ angles. Also, the thickness of the brucite-like layer of Mg/Al-LDH was 0.48 nm. After embedment of ASA into the nano-size domain of the LDH interlayers, the gallery height was modified to d_{003} = 0.98 nm (d_{006} = 0.49 nm) by subtracting the thickness of LDHs layer (0.98-0.48 nm = 0.50 nm) from its d_{003}.

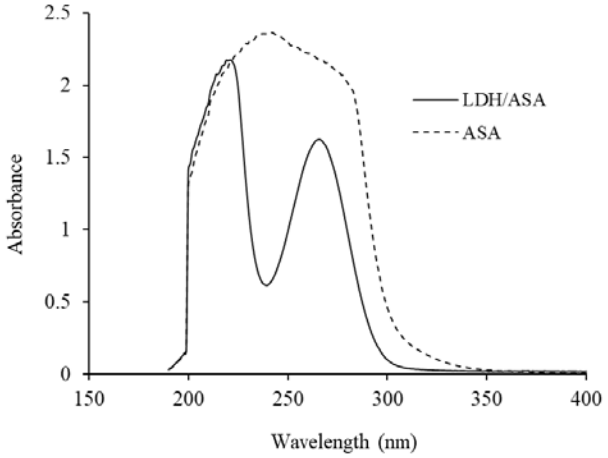

Fig. 1. UV-visible absorption spectra of ASA and LDH-ASA. ASA; Ascorbic acid; LDH, layered double hydroxides.

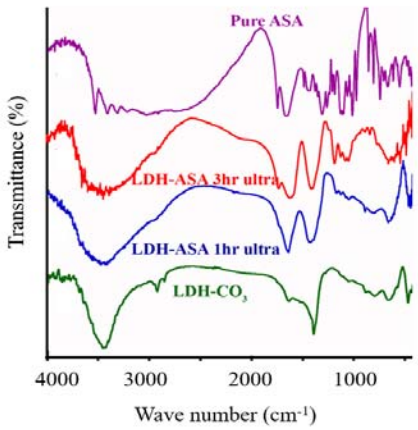

Fig. 2. Fourier-transform infrared spectrum of neat ASA, LDH-ASA 3 h ultra, LDH-ASA 1 h ultra, and LDH-CO_3. ASA, Ascorbic acid; LDH, layered double hydroxides.

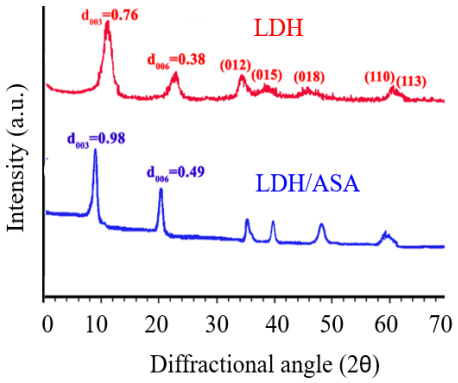

Fig. 3. X-ray diffraction pattern of the neat LDH and LDH/ASA with 3 h ultrasonic irradiation. ASA, Ascorbic acid; LDH, layered double hydroxides.

Morphology characterization of the Mg/Al-ASA LDHs was performed by TEM and FE-SEM at different ultrasonic treatment times as shown in Figs. 4 and 5.

The thermal behavior of the Al/Mg-LDH and LDH-ASA system were examined by TGA analysis to determine the degradation temperature and the interacted anion amount under the N_2 atmosphere (Fig. 6).

The results of ICP analysis showed that the atomic Mg^{2+}/Al^{3+} ratio in the prepared samples was close enough to the 2:1 ratio of the co-precipitation method. Moreover, the general formula of the synthesized LDH-ASA was determined by simultaneous considering of the CHNS analysis and TGA results. According to the CHNS results, the experimental weight contents of C, H, and N are 18.93, 3.89, and 2.57, respectively. Based on the general formula of LDH materials and element analysis data of carbon, the degree of intercalation of ASA was estimated as 91%. Accordingly, the ideal formula of Mg/Al-ASA LDH is deduced as $Mg_2Al(OH)_6(ASA)_{0.91}(NO_3^{2-})0.4H_2O$.

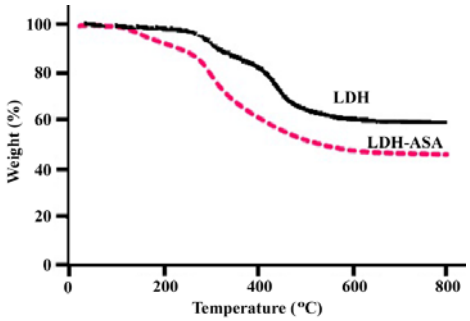

Fig. 6. Thermogravimetric analysis curves of Al/Mg-LDH and LDH-ASA system with 3h ultrasonic irradiation. ASA, Ascorbic acid; LDH, layered double hydroxides.

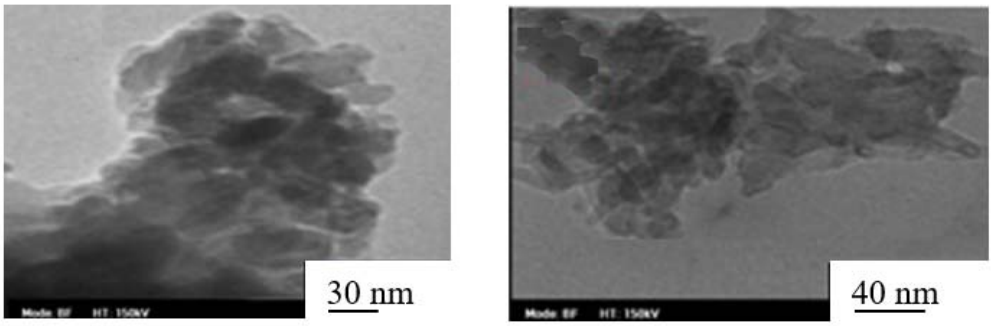

Fig. 4. Transmission electron microscopy of Mg/Al-ASA LDH with 3 h ultrasonic irradiation.

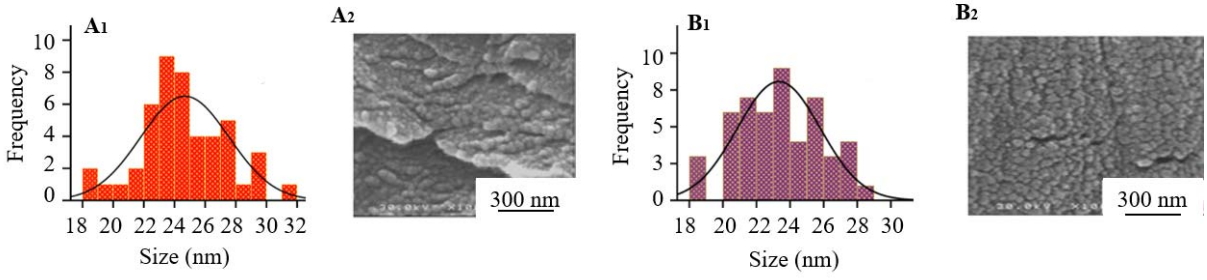

Fig. 5. Field emission scanning electron microscopy and corresponding particle size distribution histograms of (A) the Mg/Al- ascorbic acid layered double hydroxides with 1 h ultra and (B) 3 h ultrasonic irradiation.

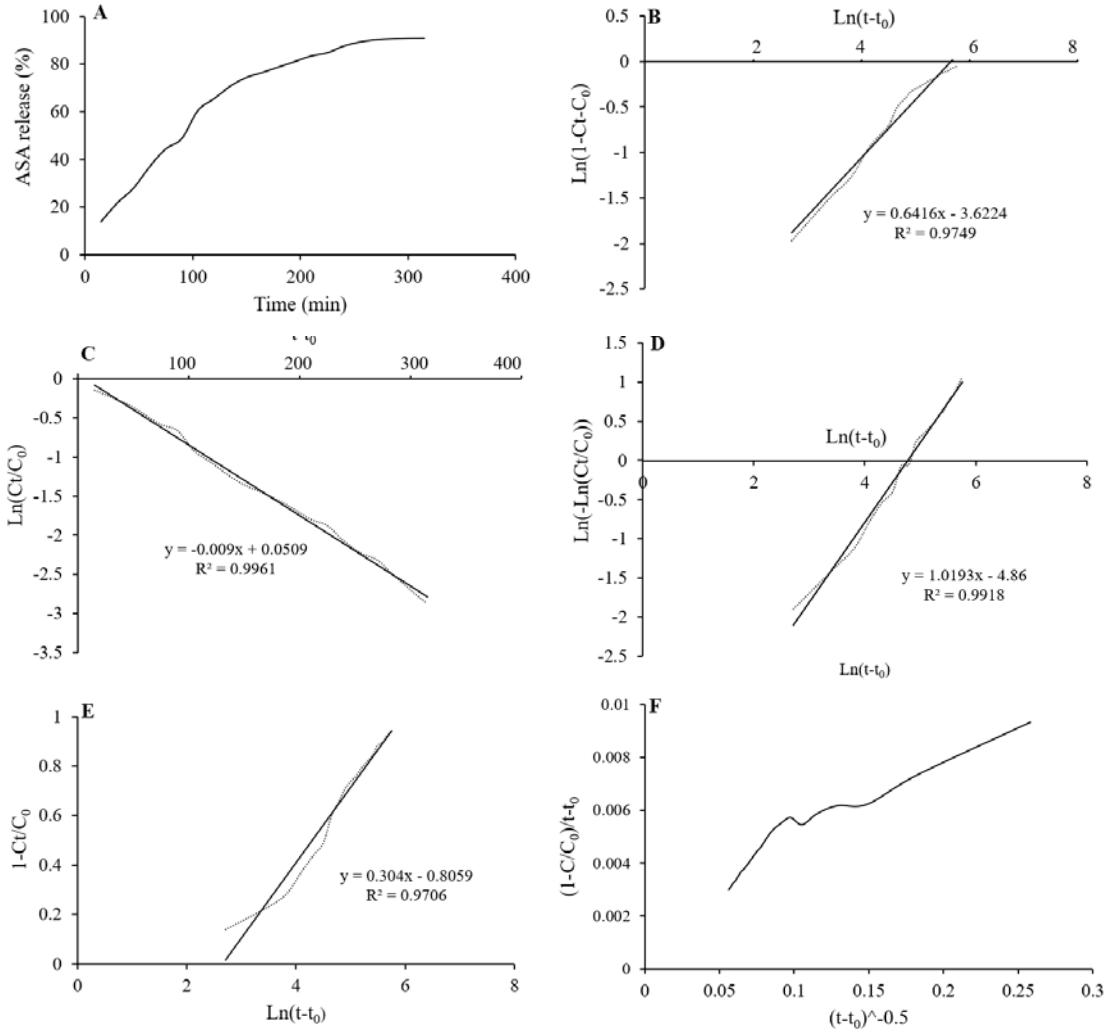

Fig. 7. (A) Deintercalation of the ASA in concentrations 0.05 M of the Na_2CO_3 aqueous solution for periods of up to 315 min and linear fitting of various models to the release of ASA fits by (B) the modified Freundlich equation, (C) the first-order rate model, (D) the Avrami-Erofe'ev model, (E) the Elovich model, and (F) the parabolic diffusion equation. ASA, Ascorbic acid.

Deintercalation of the ASA-Mg-Al hybrids was performed at 0.05 M of the Na_2CO_3 aqueous solution for periods up to 315 min. After the required time interval, the product was filtered, and the concentration of ASA in the filtrate collected was estimated by UV-Vis spectra at a wavenumber of 265 nm. The curves related to the kinetic profile of intercalated ASA and its fitted models are shown in Fig. 7.

DISCUSSION

One of the most straightforward ways for inserting organic anion species into the interlayer spacing LDHs is one step co-precipitation method. In this method, the excess positive charge in formulas was compensated by nitrate, ascorbic anions, and water molecular present in the interlayer region (Scheme 1). In LDHs, a steady-state of crystal structure was attained by electrostatic interactions and hydrogen bonds between the host cationic brucite-like layers and the contents of the gallery, which keep the layers together. The spectrum of pure sodium ASA revealed one strong absorption at 265 nm belonging to π-π^* transition (22). A similar strong absorption peak at 265 nm (Fig. 1) was observed for Mg/Al-LDH ASA, confirming the presence of ASA anion in LDHs.

According to FT-IR analysis, in the spectrum of Mg/Al-LDH broad bands in the 3460 and 1625 cm^{-1} are associated with stretching and deformation vibration of hydroxyl basal layer and interlayer H_2O molecules. The bands at 1383 and 783 cm^{-1} are associated with the asymmetric stretching and out-of-plane deformation of the nitrate anion and carbonate groups (CO_3^{2-}) in the layers. Absorption occurring below the 1000 cm^{-1} region is attributed to metal oxide stretching within the LDH basal layer. The recorded FT-IR spectrum of neat ASA showed absorption peaks in regions of 1672 cm^{-1} (C=O), 1672-1497 cm^{-1} (conjugate C=C), 1363 cm^{-1} (C-O-C), and 1321 cm^{-1} (C-O). After ultrasonic irradiation at different treatment times, Mg/Al-ASA LDH spectra were indicated characteristic bands of ASA with the minor changes in the intensity of the absorption band, which confirmed the presence of ASA molecules within LDH layers. Moreover, somewhat shifted in absorption bands toward higher wavenumbers possibly are corresponded to the intramolecular H-bonds and electrostatic interaction between negative ASA and positive LDH basal layer, to suggest their safe stabilization in the interlayer space of LDH. As shown in Fig. 2, by increasing the reaction time from 1 h to 3 h under ultrasonic irradiation, the amount of ASA in hybrid was increased, so it was used for further investigation.

The XRD pattern of the neat LDH and LDH/ASA samples showed the hydrotalcite-like characteristic reflections of d_{003} = 0.76 and d_{006} = 0.38 nm peaks (Fig. 3), which can be indicated well-stacked lamellar structure and confirmed that the structure of the LDHs is not destroyed after sonication. In the case of Mg/Al-ASA LDH, sharp and symmetric (003) and (006) Bragg reflection shifts to lower 2θ angles confirmed the interaction of ASA with hydroxides and decreases the crystallinity of LDH structure. Also, inserted ASA into the gallery space of LDH caused the increase of the interlayer distance and the growth of basal spacing. The crystallographic structure of the LDH-ASA is schematically shown in Scheme 1. According to a previous report (24), the molecular size of ASA is estimated at 0.49, 0.60, and 0.36 nm in length, width, and thickness, respectively. The thickness of the brucite-like layer of Mg/Al-LDH is 0.48 nm. After embedment ASA into the nano-size domain of the LDH interlayers, the gallery height was modified to d_{003} = 0.98 nm (d_{006} = 0.49 nm) by subtracting the thickness of LDHs layer (0.98 - 0.48 nm = 0.50 nm) from its d_{003}, this displacement suggesting that the framework of the ASA oriented in a perpendicular direction from the backbone of the hydroxide sheets.

TEM images of Mg/Al-ASA LDH with 3 h ultra showed that Mg/Al-ASA LDH nanoflakes with a well-order layer-by-layer structure are nanoscaled. These images point to the LDH platelets with a mean diameter of 25 nm and somewhat rounded and irregularly shaped particles were dispersed (Fig. 4). The surface morphology of the Mg/Al-ASA LDHs at different treatment times and corresponding particle size distribution histograms of them were investigated by FE-SEM, as shown in Fig. 5A and B. FE-SEM micrograph related to Mg/Al-LDH-ASA with 1 h ultra demonstrated that the globular particle was distributed in surface organoclay platelets in a mean range of 24 nm. Figure 5B showed that after 3 h ultrasonic irradiation, particles with different morphology were wholly dispersed in the surface sheet. Furthermore, this work found that the degree of particles' dispersion is influenced by the function of treatment times, and dispersion of ASA into LDH apace can be improved by increasing the sonication treatment times.

The results of ICP analysis indicated that the atomic Mg^{2+}/Al^{3+} ratio in the prepared samples was close enough to the 2:1 ratio of the co-precipitation method. Moreover, the general formula of the synthesized LDH-ASA was determined by simultaneous considering of the ICP and TGA results. The thermal behavior of the Al/Mg-LDH and LDH-ASA system were examined by TGA analysis to the determination of the degradation temperature and the interacted anion amount under the N_2 atmosphere. According to Fig. 6, both samples have exhibited three steps decomposition events of a hydrotalcite-like phase with progressive mass losses in the TGA curve. The first step with mass loss below about 130 °C is

associated with the removal of physisorbed water from the external surface of the crystallites, and the second mass loss around 200-300 °C is probably corresponded to the dehydroxylation of the hydroxide sheets, together with the removal of water molecules bonded from the interlayer. The last mass loss is started around 250 °C, is attributed to the combustion of the organic anions present in the interlayer space, and extends up to 500 °C. The obtained results from the mass losses indicated that there is an acceptable agreement with element chemical analysis data.

Biomolecules are well stabilized in LDH lattice by both electrostatic and lateral interactions not only in interlayer space but also at the surface site of the host and in exceptional condition can be deintercalated by ion-exchange reaction with other anion or atmospheric CO_2. These features will allow LDHs to be applied as new drug carriers.

The release percentage of the intercalated ASA was studied at 0.05 M of the Na_2CO_3 aqueous solution for periods of up to 315 min at 265 nm (Fig. 7). The kinetic profile indicated that almost 60% ASA was released instantly, followed by a slower process taking place up to 315 min. The fast initial stage was assigned to release the ASA anions on the surface, and the external part of layered crystallites can be exchanged quite easily, which a burst release pattern. Following this step, the drug intra-particle from LDH crystallite was diffused to the external part and then to the solution, which results in a steady-slow release rate. The LDH crystallite size and the anion affinity for LDH production are essential factors for the controlled release of drug molecules.

To describe the kinetics of the release behavior of ASA guests from the lamellar space of LDH, we have attempted to fit the measured data with the following five commonly used models (22,23).

A first-order rate model has been utilized widely in the ion exchange reaction or adsorption process and can be expressed as the following equation:

$$\ln (C_t / C_0) = -K_d t \quad (1)$$

A parabolic diffusion equation has been applied to illustrate diffusion-controlled phenomena in hydroxide layers:

$$(1-C_t / C_0) /t = K_d t^{(-0.5)} + a \quad (2)$$

A modified Freundlich equation can be expressed as the following equation:

$$\ln (1- C_t / C_0) = \ln (K_d) + a \ln (t) \quad (3)$$

Which has been used to experimental data on ion exchange or release with clays by many researchers.

An Elovich model was used to study the sorption of ASA into clays sheet:

$$1- C_t / C_0 = a \ln (t) + b \quad (4)$$

An Avrami-Erofe'ev model:

$$\ln (-\ln (1-\alpha)) = n \ln (Kd) + n \ln (t) \quad (5)$$

In each equation, C_0 and C_t is the total amount of incorporated ASA in the hybrid at zero time and *t,* respectively, and the rate of release was represented by k_d, respectively. A, b, and n are specific constants of the mathematical used models and α is the extent of reaction.

It can be seen from Fig. 7 that first-order rate, Avrami-Erofe'ev, and somewhat modified Freundlich models can be used to describe the kinetics of release of ASA. In these models, according to the visual inspection of these "linear" plots and R_2 values, it appears that the first-order rate model is the most appropriate for describing the release of ASA. The values of K_d may be determined from the slope of the fitted plots which is equal to -0.009. In the first-order rate model, changes in concentration related to the time are dependent only on concentration. On the other hand in this ASA-Mg-Al hybrids as a porous material, the amount of drug released is proportional to the amount of remaining drug in the matrix. Thus, the amount of activity released tends to decrease in function of time.

CONCLUSION

An Mg/Al-LDH layered double hydroxide containing Mg^{2+} and Al^{3+} in the brucite-like layer and ASA as counter-anion was fabricated by the coprecipitation method under fast sonochemical treatment. These hybrid organic-inorganic materials can absorb, store, and control the release of ASA by using the ability of the hydrotalcite-like anionic clay. From the results of XRD and FTIR, it can be concluded

that the ASA was successfully stabilized in the gallery of the LDH lattice through electrostatic interaction. The obtained results from FE-SEM images revealed that the morphology is significantly influenced by the sonication time of treatment. Also, the thermal behavior of Mg/Al-ASA LDH showed weight loss carried out in three steps, involving the elimination of intercalated constitution water, destruction of hydroxylate layers, and pyrolysis of intercalated organic anions. The ASA release profile indicated that the amount of drug released from the synthesized Mg/Al-ASA hybrid as a porous material, is proportional to the amount of remaining drug in the matrix and the first-order rate model is the most appropriate for describing the release from Mg/Al-LDH.

Conflict of interest statement

The authors declared no conflicts of interest in this work.

Authors' contribution

P. Asadi contributed to supervision, visualization, conceptualization, validation, formal analysis, investigation, and writing the original draft of the manuscript; E. Khodamoradicontributed to writing the manuscript and investigation; M. Dinari contributed to the project administration, writing, and editing the manuscript. The final version of the manuscript was approved by all authors.

REFERENCES

1. Dinari M, Haghighi A, Asadi P. Facile synthesis of ZnAl-EDTA layered double hydroxide/poly (vinyl alcohol) nanocomposites as an efficient adsorbent of Cd (II) ions from the aqueous solution. Appl Clay Sci. 2019;170:21-28. DOI: 10.1016/j.clay.2019.01.007.
2. Evans GD. Slade RCT. Structural aspects of layered double hydroxides. Struct Bond. 2006;119:1-87. DOI: 10.1007/430_005.
3. Rousselot I, Guého CT, Leroux F, Léone P, Palvadeau P, Besse JP. Insights on the structural chemistry of hydrocalumite and hydrotalcite-like materials: investigation of the series $Ca^2M^{3+}(OH)_6Cl\cdot 2H_2O$ (M^{3+}: Al^{3+}, Ga^{3+}, Fe^{3+}, and Sc^{3+}) by X-ray powder diffraction. J Solid State Chem. 2002;167(1):137-144. DOI: 10.1006/jssc.2002.9635.
4. Cavani F, Trifirò F, Vaccari A. Hydrotalcite-type anionic clays: preparation, properties and applications. Catal Today. 1991;11(2):173-301. DOI: 10.1016/0920-5861(91)80068-K.
5. Samuei S, Fakkar J, Rezvani Z, Shomali A, Habibi B. Synthesis and characterization of graphene quantum Dots/CoNiAl-layered double-hydroxide nanocomposite: application as a glucose sensor. Anal Biochem. 2017;521:31-39. DOI: 10.1016/j.ab.2017.01.005.
6. Ferrer DI. Supported Layered Double Hydroxides as CO2 Adsorbents for Sorptionenhanced H2 Production. Chemical Engineering, Imperial College, London, United Kingdom: Springer, International Publishing Switzerland; 2016. pp: 209. DOI: 10.1007/978-3-319-41276-4.
7. Chen Y, Shui Z, Chen W, Chen G. Chloride binding of synthetic Ca-Al-NO3 LDHs in hardened cement paste. Constr Build Mater. 2015;93:1051-1058. DOI: 10.1016/j.conbuildmat.2015.05.047.
8. Rahmanian O, Amini S, Dinari M. Preparation of zinc/iron layered double hydroxide intercalated by citrate anion for capturing Lead (II) from aqueous solution. J Mol Liq. 2018;256:9-15. DOI: 10.1016/j.molliq.2018.02.018.
9. Dinari M, Dadkhah F. Swift reduction of 4-nitrophenol by easy recoverable magnetite-Ag/layered double hydroxide/starch bionanocomposite. Carbohydrate Polym. 2020;228:115392,1-8. DOI: 10.1016/j.carbpol.2019.115392.
10. Rahmanian O, Dinari M, Abdolmaleki MK. Carbon quantum dots/layered double hydroxide hybrid for fast and efficient decontamination of Cd (II): the adsorption kinetics and isotherms. Appl Sur Sci. 2018;428:272-279. DOI: 10.1016/j.apsusc.2017.09.152.
11. Kim TH, Oh JM. Dual nutraceutical nanohybrids of folic acid and calcium containing layered double hydroxides. J Solid State Chem. 2016;233:125-132. DOI: 10.1016/j.jssc.2015.10.019.
12. Chakraborti M, Jackson JK, Plackett D. The application of layered double hydroxide clay (LDH)-poly(lactide-*co*-glycolic acid) (PLGA) film composites for the controlled release of antibiotics. J Mater Sci: Mater Med. 2012;23(7):1705-1713. DOI: 10.1007/s10856-012-4638-y.
13. Silion M, Hritcu D, Lisa G, Popa IM. New hybrid materials based on layered double hydroxides and antioxidant compounds. Preparation, characterization and release kinetic studies. J Porous Mater. 2012;19:267-276. DOI: 10.1007/s10934-011-9473-x.
14. Aisawa S, Ohnuma Y, Hirose K, Takahashi S, Hirahara H, Narita E. Intercalation of nucleotide for layered double hydroxides by ionexchange reaction. Appl Clay Sci. 2005;28(1-4):137-145. DOI: 10.1016/j.clay.2004.01.008.
15. Aisawa S, Kudo H, Hoshi T, Takahashi S, Hirahara H, Umetsu Y, *et al*. Intercalation behavior of amino acids into Zn-Al layered double hydroxide by

calcination-rehydration reaction. J Solid State Chem. 2004;177(11):3987-3994.
DOI: 10.1016/j.jssc.2004.07.024.
16. Konari M, Heydari-Bafrooei E, Dinari M. Efficient immobilization of aptamers on the layered double hydroxide nanohybrids for the electrochemical proteins detection. Int J Biol Macromol. 2021;166:54-60.
DOI: 10.1016/j.ijbiomac.2020.10.063.
17. Mishra G, Dash B, Pandey S. Layered double hydroxides: a brief review from fundamentals to application as evolving biomaterials. Appl Clay Sci. 2018;153:172-186.
DOI: 10.1016/j.clay.2017.12.021.
18. Forano C, Costantino U, Prévot V, Taviot Gueho C. Layered double hydroxides (LDH). In: Bergaya F, Lagaly G. editors. Handbook of Clay Science. 2nd ed. Part A: Fundamentals, Developments in Clay Science. 2013;5:745-782.
DOI: 10.1016/B978-0-08-098258-8.00025-0.
19. Saifullah B, Hussein MZ, Hussein-Al-Ali SH, Arulselvan P, Fakurazi S. Antituberculosis nanodelivery system with controlled-release properties based on para-amino salicylate-zinc aluminum-layered double-hydroxide nanocomposites. Drug Des Dev Ther. 2013;7:1365-1375.
DOI: 10.2147/DDDT.S50665.
20. Rives V, del Arco M, Martín C. Intercalation of drugs in layered double hydroxides and theircontrolled release: a review. Appl Clay Sci. 2014;88-89:239-269.
DOI: 10.1016/j.clay.2013.12.002.
21. Pillai SK, Kleyi P, Beer MD, Mudaly P. Layered double hydroxides: an advanced encapsulation and delivery system for cosmetic ingredients-an overview. Appl Clay Sci. 2020;199:105868.
DOI: 10.1016/j.clay.2020.105868.
22. Gao X, Chenb L, Xie J, Yin Y, Chang T, Duan Y, *et al*. *In vitro* controlled release of vitamin C from Ca/Al layered double hydroxide drug delivery system. Mater Sci Eng C. 2014;39:56-60.
DOI: 10.1016/j.msec.2014.02.028.
23. Gasser MS. Inorganic layered double hydroxides as ascorbic acid (vitamin C) delivery system-intercalation and their controlled release properties. Colloids Surf B: Biointerfaces. 2009;73:103-109.
DOI: 10.1016/j.colsurfb.2009.05.005.
24. Gao X, Lei L, Hare DO, Xie J, GaoP, Chang T. Intercalation and controlled release properties of vitamin C intercalated layered double hydroxide. J Solid State Chem. 2013;203:174-180.
DOI: 10.1016/j.jssc.2013.04.028.
25. Aguilera MV, Galvez D, Sanchez C, Herrera-Ceballos E. Changes in photoinduced cutaneous erythema with topical application of a combination of vitamins C and E before and after UV exposure. J Dermatol Sci. 2012;66(3):216-220.
DOI: 10.1016/j.jdermsci.2012.03.010.
26. Talaulikar VS, Manyonda IT. Vitamin C as an antioxidant supplement in women's health: a myth in need of urgent burial. Eur J Obstet Gynaecol Reprod Biol. 2011;157(1):10-13.
DOI: 10.1016/j.ejogrb.2011.03.017.
27. Chikvaidze E, Topeshashvili M. Effect of ascorbic acid (vitamin C) on the ESR spectra of the red and black hair: pheomelanin free radicals are not always present in red hair. Magn Reson Chem. 2015;53(12):1019-1023.
DOI: 10.1002/mrc.4291.
28. Zielinski H, Kozlowska H, Lewczuk B. Bioactive compounds in the cereal grains before and after hydrothermal processing. Innov Food Sci Emerg Technol. 2001;2(3):159-169.
DOI: 10.1016/S1466-8564(01)00040-6.
29. Shafiei SS, Solati-Hashjin M, Rahim-Zadeh H, Samadikuchaksaraei A. Synthesis and characterisation of nanocrystalline Ca-Al layered double hydroxide {$[Ca_2Al(OH)_6]NO_3.nH_2O$}: *in vitro* study. Adv Appl Ceram. 2013;112(1):59-65.
DOI: 10.1179/1743676112Y.0000000045.
30. Khan AI, Lei L, Norguist AJ, Ohare D. Intercalation and controlled release of pharmaceutically active compounds from a layered double hydroxide. Chem Comm (Camb). 2001;22:2342-2243.
DOI: 10.1039/b106465g.
31. Hayati P, Rezvani AR, Morsali A, Retailleau P. Ultrasound irradiation effect on morphology and size of two new potassium coordination supramolecule compounds. Ultrason Sonochem. 2017;34:195-205.
DOI: 10.1016/j.ultsonch.2016.05.031.
32. Dinari M, Mallakpour Sh. Ultrasound-assisted one-pot preparation of organomodified nano-sized layered double hydroxide and its nanocomposites with polyvinylpyrrolidone. J Polym Res. 2014;21(2):350-357.
DOI: 10.1007/s10965-013-0350-y.
33. Soltani R, Shahvar A, Dinari M, Saraji M. Environmentally-friendly and ultrasonic-assisted preparation of two-dimensional ultrathin Ni/Co-NO3 layered double hydroxide nanosheet for micro solid-phase extraction of phenolic acids from fruit juices. Ultrason Sonochem. 2018;40(Pt A):395-401.
DOI: 10.1016/j.ultsonch.2017.07.031.
34. Dinari M, Haghighi A. Ultrasound-assisted synthesis of nanocomposites based on aromatic polyamide and modified ZnO nanoparticle for removal of toxic Cr(VI) from water. Ultrason Sonochem. 2018;41:75-84.
DOI: 10.1016/j.ultsonch.2017.09.023.
35. Ezeha CI, Tomatisa M, Yanga X, Hea J, Sun C. Ultrasonic and hydrothermal mediated synthesis routes for functionalized Mg-Al LDH: comparison study on surface morphology, basic site strength, cyclic sorption efficiency and effectiveness. Ultrason Sonochem. 2018;40(Pt A):341-352.
DOI: 10.1016/j.ultsonch.2017.07.013.